Theoretical study of quadratic electro-optic effect in semiconducting zigzag carbon nanotubes

Abbas Zarifi,* Christian Fisker, and Thomas Garm Pedersen
Department of Physics and Nanotechnology, Aalborg University, Skjernvej 4A, DK-9220 Aalborg East, Denmark
(Received 14 March 2007; published 6 July 2007)

Using the perturbation treatment developed by Aspnes and Rowe [Phys. Rev. B **5**, 4022 (1972)], an analytic expression for the third-order nonlinear optical susceptibility $\chi^{(3)}(\omega;0,0,\omega)$ is computed and analyzed for single walled zigzag carbon nanotubes. By improving their method, our calculations based on a tight-binding model take into account the transitions between all pairs of valence and conduction bands and thereby the contributions to the third-order susceptibility associated with different energy bands are investigated. With increasing radius of the nanotube, a nonmonotonous increase of the quadratic electro-optic effect has been demonstrated except for the fundamental peak. The nonuniformity is a result of the overlap between two energy bands as well as the reduced effective masses associated with each pair of conduction and valence bands. A nonperturbative numerical calculation is applied to obtain the high-field response as well as to assess the applicability of the low-field perturbation expression.

DOI: 10.1103/PhysRevB.76.045403 PACS number(s): 78.67.Ch, 78.20.−e

I. INTRODUCTION

The physical properties of carbon nanotubes (CNs), as quasi-one-dimensional systems, have been intensively studied theoretically and experimentally.[1–8] Of considerable interest are the nonlinear optical (NLO) properties of semiconductor CNs not only because the nonlinear spectrum gives information on their electronic structure but also in view of the possible device applications. Along with third-harmonic generation, electro-optic (EO) or dc Kerr effect studies have been used to investigate the origins of the optical nonlinearities in CNs as well as CN-based composite materials. Several experimental results on the NLO properties of CNs have been reported so far[9–14] and some papers have studied theoretically the third-order nonlinear optical susceptibility and EO effect in semiconducting CNs.[15–19] All previous theoretical approaches to NLO properties in CNs are based on numerical calculations and rely on the two-band approximation. In this paper, we derive an analytic expression for the third-order nonlinear optical susceptibility of semiconducting zigzag CNs in the presence of a uniform electric field directed along the nanotube axis. Our calculations are based on a tight-binding model and include all energy bands of the semiconducting zigzag CNs. Therefore, it is possible to study closely the contribution to the quadratic electro-optic (QEO) effect from different energy bands. The obtained results generally agree with those previously reported for the fundamental resonance peak. However, for higher resonance peaks, a more complicated behavior follows from our calculations. We do not see a monotonous increase of $\chi^{(3)}(\omega;0,0,\omega)$ for higher resonances.

The outline of the paper is as follows. In Sec. II, we derive an analytic expression for the QEO function of semiconducting zigzag CNs. In Sec. III, the physical reason for a nonuniform behavior of $\chi^{(3)}(\omega;0,0,\omega)$ for higher resonances is discussed. Furthermore, the apparent displacement of fundamental resonance peak between two groups of semiconducting CNs reported in some papers is analyzed and shown to be simply a question of taking an approximate rather than exact value of the band gap for semiconducting zigzag CNs. In order to obtain the high-field response and to assess the applicability of the perturbation approach, we study numerically the response of a long but finite length CN placed in a uniform electric field in Sec. IV before summarizing our conclusions in Sec. V.

II. THEORY AND ANALYTICAL DERIVATIONS

Single walled CNs, constructed by rolling up a graphite sheet into a cylinder, are characterized by two integers (n,m). For a more detailed classification of zigzag CNs ($m=0$) as a subclass of CNs, we introduce two integer parameters p and q which are connected with n by means of the relation $n=3p+q$. The zigzag tubes with $q=0$ are known as narrow gap semiconductors (metallic) whereas the tubes with $q=1,2$ and arbitrary p are moderate-gap semiconductors (MSs). Among these, the MS with index $q=1$ are defined as MS1 and those with index $q=2$ are defined as MS2. In our previous work[20] (hereafter referred to as I) using an orthogonal π-orbital tight-binding model, we obtained the electronic structure, electric dipole matrix elements, and subsequently linear susceptibility of zigzag CNs. In the present work, we obtain an analytic expression for the QEO effect in zigzag CNs. We utilize the perturbation expression obtained by Aspnes and Rowe[21] in their derivation of the third-order nonlinear optical susceptibility caused by a uniform electric field using time-dependent perturbation theory. The same method has been applied in Ref. 22 to find the QEO effect in the conjugated polymer poly(*para*-phenylene). The zz component of the EO function in the vicinity of each band gap is given by[21]

$$\chi_{zz}^{(3)}(\omega;0,0,\omega)=\frac{1}{3\hbar^2\Omega^2}\frac{e^2\hbar^2F^2}{8m^*}\frac{\partial^3[\hbar^2\Omega^2\chi_{zz}(\omega)]}{\partial(\hbar\Omega)^3}, \quad (1)$$

where $e>0$ is the elementary charge, m^* the reduced effective mass, F the dc field directed along the nanotube axis, $\hat{z}$, and where $\hbar\Omega=\hbar\omega+i\hbar\Gamma$ includes the photon energy and the phenomenological broadening parameter Γ. As in I, we have introduced the dimensionless "susceptibility" $\chi_{zz}(\omega)$ ob-

tained by normalizing the polarizability (per unit length) by the cross-sectional area $A=\pi R^2$, where $R=na/2\pi$ is the radius of a zigzag CN and a is the lattice constant of graphene. We notice that Eq. (1) only includes transitions between single pairs of bands while the linear susceptibility $\chi_{zz}(\omega)$ in our calculations includes contributions from many pairs of bands. Consequently, to include all pairs of conduction (c) and valence (v) bands, the reduced effective mass m^* associated with each pair is applied separately.

It follows from Eq. (1) that to compute $\chi_{zz}^{(3)}(\omega;0,0,\omega)$, the third derivative of $\chi_{zz}(\omega)$ with respect to Ω should be taken. However, the third derivative of the final result for the linear susceptibility obtained in I gives a rather complicated form of the QEO function. Therefore, we first derive a more useful albeit approximate form for the linear susceptibility. We start with Eq. (15) in I written in the following form:

$$\chi_{zz}^{(\mu)}=\frac{1}{6}\int_{\rho_g/2}^{\rho_0/2}\frac{\gamma_0^2\left[3\cos\left(\frac{2\mu\pi}{n}\right)+\frac{3}{2}-\frac{\rho^2}{2}\right]^2 d\rho}{\rho^2(4\rho^2\gamma_0^2-\hbar^2\Omega^2)\sqrt{\left(\rho^2-\frac{\rho_0^2}{4}\right)\left(\frac{\rho_g^2}{4}-\rho^2\right)}}, \tag{2}$$

where $\gamma_0\approx 2.89$ eV is the nearest-neighbor overlap integral and the integral bounds as normalized band-gap parameters are given by $\rho_g=2\sqrt{3+2\cos(2\mu\pi/n)-4\cos(\mu\pi/n)}$ and $\rho_0=2\sqrt{3+2\cos(2\mu\pi/n)+4\cos(\mu\pi/n)}$, defined by Eq. (13) in I, where $\mu=1,2,\ldots,n$. A factor of 1/6 was missing in Eq. (15) in I due to a typographical error. In evaluating the linear susceptibility on the basis of Eq. (2), we apply the following approximate method. First, we note the fact that

$$\begin{cases}\rho_0>\rho_g & \text{if } 1\leqslant\mu\leqslant(n-1)/2\\ \rho_0<\rho_g & \text{if } (n+1)/2\leqslant\mu\leqslant n\end{cases}\quad\text{for odd } n,$$

$$\begin{cases}\rho_0>\rho_g & \text{if } 1\leqslant\mu\leqslant(n-2)/2\\ \rho_0<\rho_g & \text{if } (n+2)/2\leqslant\mu\leqslant n\\ \rho_0=\rho_g & \text{if } \mu=n/2\end{cases}\quad\text{for even } n. \tag{3}$$

Hence, in the case $\rho_0<\rho_g$, the factor $\sqrt{\rho_g^2/4-\rho^2}$ in Eq. (2) can be approximated by $\rho_g/2$ since ρ is much smaller than ρ_g in the dominant part of the integration. After introducing this approximation, Eq. (2) finally yields the following analytic result for the long-axis linear susceptibility of zigzag CNs. For odd n,

$$\chi_{zz}(\omega)=\frac{4e^2a}{\sqrt{3}\pi\varepsilon_0A\gamma_0}\left[\sum_{\mu=(n+1)/2}^{n-1}\chi_{zz}^{(\mu)}(\omega)+\chi_{zz}^{(n)}(\omega)/2\right], \tag{4}$$

and for even n,

$$\chi_{zz}(\omega)=\frac{4e^2a}{\sqrt{3}\pi\varepsilon_0A\gamma_0}\left[\sum_{\mu=(n+2)/2}^{n-1}\chi_{zz}^{(\mu)}(\omega)+\chi_{zz}^{(n)}(\omega)/2+\chi_{zz}^{(n/2)}(\omega)\right]. \tag{5}$$

Here,

$$\chi_{zz}^{(\mu)}(\omega)=\frac{-3\gamma_0^2\sqrt{\rho_g^2-\rho_0^2}}{32\rho_g^2\rho_0^2\hbar^2\Omega^2}(\rho_g^2+\rho_0^2-16)^2+\frac{iy^2}{24\rho_g\hbar^3\Omega^3}\frac{\arctan(u)}{x^{1/2}},\quad \mu\neq n/2 \tag{6}$$

and

$$\chi_{zz}^{(n/2)}(\omega)=\frac{\pi\gamma_0^2}{3(4\gamma_0^2-\hbar^2\Omega^2)}, \tag{7}$$

where

$$y=3\gamma_0^2(\rho_g^2+\rho_0^2-16)/2-\hbar^2\Omega^2,$$

$$x=\hbar^2\Omega^2-\rho_0^2\gamma_0^2,$$

$$u=i\hbar\Omega x^{-1/2}\sqrt{1-(\rho_0/\rho_g)^2}. \tag{8}$$

Above, ε_0 is the vacuum permittivity. In Eq. (6), a small frequency-independent term has been ignored since it makes a vanishing contribution to the QEO function. The simplified expression obtained for the linear susceptibility of semiconducting zigzag CNs is in excellent agreement with the full expression, Eq. (16), obtained in I. Introducing the results of Eqs. (4)–(7) into Eq. (1), one obtains the QEO function. It is noticed that upon multiplication by $\hbar^2\Omega^2$, the first term of Eq. (6) becomes independent of $\hbar\Omega$ and thus its derivative is zero. In addition, we find an infinite effective mass for the flat energy bands associated with $\mu=n/2$ and consequently a vanishing nonlinear susceptibility. Therefore, the only nonzero contribution to Eq. (1) comes from the second term of Eq. (6).

For the calculation of $\chi^{(3)}(\omega;0,0,\omega)$, we need the reduced effective mass related to each pair of c and v bands. According to the tight-binding model, the band gaps and the reduced effective masses for a $(n,0)$ CN are given by $E_g=2\gamma_0|1+2\cos(\pi\mu/n)|$ and $m_\mu^*=\hbar^2/(3\gamma_0a^2)\times|2+1/\cos(\pi\mu/n)|$, respectively, where $\mu=1,2,\ldots,n$. The values of μ for the fundamental band gap (Δ_g) of each CN are given by $\mu=(2n+1)/3$ and $(2n-1)/3$ for MS1 and MS2, respectively.[23] After using the only nonzero term of Eq. (6) as well as the obtained reduced effective mass and assuming that the slowly varying factors are constant during differentiation, one obtains the following result

$$\chi_{zz}^{(3)}(\omega;0,0,\omega)\simeq\frac{ie^4aF^2}{12\sqrt{3}\varepsilon_0n^2}\left[\sum_{\mu=n'}^{n-1}G^{(\mu)}(\omega)+G^{(n)}(\omega)/2\right], \tag{9}$$

where $n'=(n+2)/2$ and $(n+1)/2$ for semiconducting zigzag CNs with even and odd n, respectively, and the function $G^{(\mu)}(\omega)$ is given by

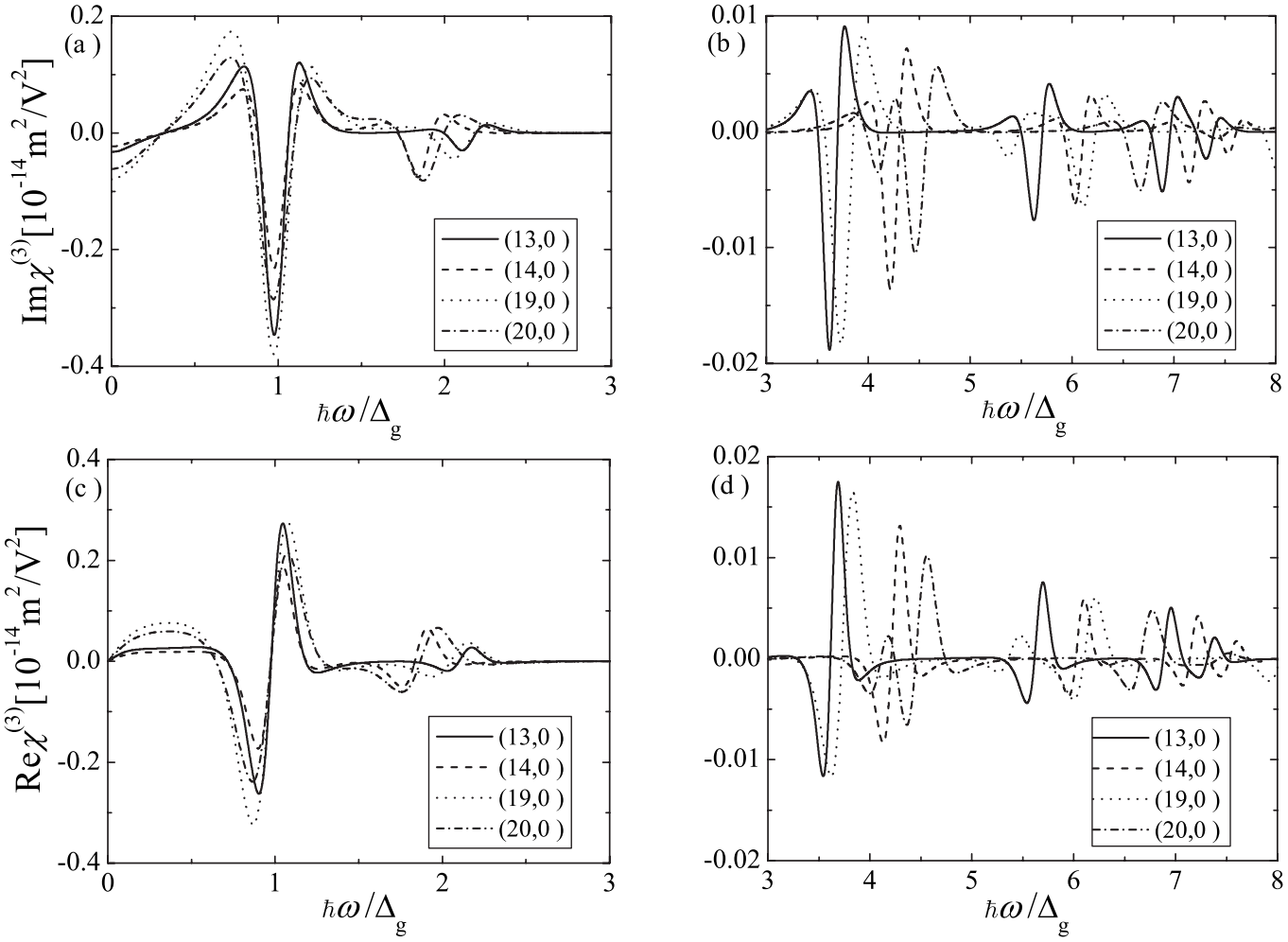

FIG. 1. Frequency dependence of $\chi^{(3)}(\omega;0,0,\omega)$ for four different CNs. In panels (a) and (c), the two lowest resonances are shown and the higher resonances are illustrated in panels (b) and (d) using a different scale.

$$G^{(\mu)}(\omega) = \frac{-y^2x^{-7/2}(\hbar\Omega)^{-6}}{\rho_g|2+1/\cos(\pi\mu/n)|}\Bigg\{\arctan(u)[6x^3+3x^2(\hbar\Omega)^2 + 15(\hbar\Omega)^6] + \frac{8u^5}{(1+u^2)^3}\rho_0^6\gamma_0^6 - \frac{2u^3}{(1+u^2)^2}[2x^3 + 9x^2(\hbar\Omega)^2 - 24x(\hbar\Omega)^4 + 13(\hbar\Omega)^6] - \frac{u}{1+u^2}[6x^3 + 3x^2(\hbar\Omega)^2 + 24x(\hbar\Omega)^4 - 33(\hbar\Omega)^6]\Bigg\}. \quad (10)$$

Together with Eq. (9), this relatively simple equation allows us to compute analytically the QEO function for all semiconducting zigzag CNs while still including transitions between all pairs of valence and conduction bands. Importantly, as shown in Eq. (10), the position and magnitude of resonances associated with different transitions are accounted for by using separate band gaps and effective masses for each term.

III. RESULTS AND DISCUSSION

The imaginary (Im) and real (Re) parts of $\chi^{(3)}(\omega;0,0,\omega)$ for some semiconducting zigzag CNs are illustrated in Fig. 1, where the broadening parameter $\hbar\Gamma = 0.15$ eV. A monotonous increase of the third-order optical nonlinearity as well as QEO effect with the increasing CN radius has been reported in Refs. 15, 16, and 19 and some papers have reported a monotonous increase within each group of MS1 and MS2.[18,24] In fact, this is not the case for all resonance peaks. For example, the graphs plotted in Fig. 1 demonstrate that the magnitude of the third resonance peak around $\hbar\omega = 4\Delta_g$ of (14,0) is much larger than that of (20,0). This difference can be understood from the band structure of the two species. Thus, the large magnitude resonance peak of the (14,0) nanotube can be attributed to a near degeneracy between third and fourth bands (counted from the Fermi level) at $k=0$ as well as a small effective mass of the fourth energy band. The same is the case for the fourth resonance peak of (13,0) illustrated in Fig. 1 for $\hbar\omega$ between 5 and $6\Delta_g$, which is much larger than that of (19,0) as a result of the overlap between the fourth and fifth energy bands around $k=0$ as well as the small effective mass of the fifth energy band. Thereby, the difference between magnitudes of the first resonance peaks for the two MS groups with nearly the same radius is reasonable. By considering the values of μ for the highest v band and lowest c band, it is found that the effec-

tive mass of MS1 is smaller than that of MS2 and, besides, the dipole matrix elements of MS1 are larger than those of MS2, when they have nearly the same radius. Therefore, they result in a very pronounced peak of $\chi^{(3)}(\omega;0,0,\omega)$ for MS1. Again, we notice that this is not the case for all resonance peaks. For example, as shown in Fig. 1, the magnitude of the second peak of MS2 is larger than that of MS1, because of the smaller effective mass and larger dipole matrix elements associated with the second v band and c band of MS2 in comparison with that of MS1. All in all, except for the fundamental resonance, we do not see a monotonous increase of QEO effect with increasing tube radius.

When plotted as a function of the normalized photon energy $\hbar\omega/\Delta_g$, the fundamental resonance is expected to be at an identical position for all CNs. However, a displacement of the $\chi^{(3)}(\omega;0,0,\omega)$ resonance peaks of MS1 with respect to those of MS2 has been reported in Ref. 18. The authors claimed that the shift resulted from the curvature effects and π-σ hybridization. The same displacement has been reported in Ref. 24 in a theoretical study of the third-order nonlinearity in CNs exposed to intensive electromagnetic fields based on a perturbative and a nonperturbative model. We express that this is not a characteristic feature of these two groups of semiconducting CNs. The reason for the apparent displacement is simply that an approximate rather than exact value of the band gap has been applied. In both papers, the dispersion energy as well as electric dipole matrix elements are obtained based on a tight-binding model and then to normalize the photon energy with the band gap, the authors of Refs. 18 and 24 have taken an approximate value of the band gap given by $2\gamma_0\pi/\sqrt{3}n$. If the exact value of the band gap obtained by the tight-binding model is used, as in the present work and in Ref. 23, no shift will appear as is apparent from Fig. 1. By taking the approximate value of the band gap, the same shift of $\approx$0.03 appears in our plots, which do not contain the curvature effects or π-σ hybridization. In addition, an incorrect factor of 4 has been included in the second term of the transition matrix elements by Xu and Xiong,[17,18] which changes the transition matrix elements for zigzag CNs appreciably. Therefore, using this form of transition matrix elements, one cannot get a reliable result for QEO function. Regarding the second and higher resonances, the peaks appear at different positions for different CNs even when plotted versus the normalized photon energy $\hbar\omega/\Delta_g$.

To show the limiting behavior of the QEO effect with increasing CN radius, Fig. 2 illustrates that the imaginary and real parts of $\chi^{(3)}(\omega;0,0,\omega)$ of (38,0) and (50,0) CNs belonging to MS2 display an equal peak magnitude. By considering CNs with even larger radii, we observed a decrease in the magnitude of the QEO effect.

IV. NUMERICAL RESULTS

For comparison with the analytical result, a numerical tight-binding calculation is made as well. A long nanotube is modeled as a sequence of N unit cells and a constant electric field $\vec{F}=F\hat{z}$ is applied in the direction of the nanotube axis. The elements of the $4nN\times 4nN$ dimensional Hamiltonian matrix are defined by

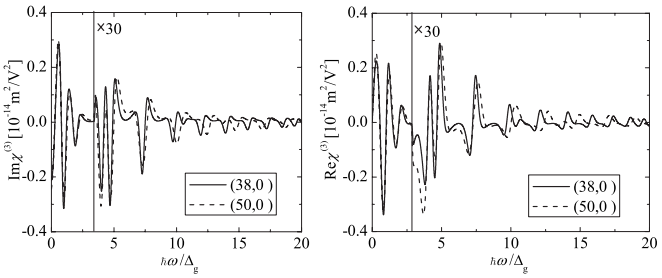

FIG. 2. Frequency dependence of $\chi^{(3)}(\omega;0,0,\omega)$ for (38,0) and (50,0) zigzag CNs. The rightmost part of the plots has been multiplied by a factor of 30.

$$H_{ij}=\begin{cases}-eFz_i & \text{if } i=j\\ \gamma_0 & \text{if } i \text{ and } j \text{ are nearest neighbors}\\ 0 & \text{otherwise.}\end{cases} \quad (11)$$

The third-order nonlinear optical susceptibility in the weak-field limit is approximated as

$$\Delta\chi(\omega;0,0,\omega)\approx\frac{\chi(F,\omega)-\chi(0,\omega)}{F^2}. \quad (12)$$

Using molecular electronic states $\Phi(\vec{r})$, the field-dependent susceptibility $\chi(F,\omega)$ is defined as

$$\chi(F,\omega)=\frac{2e^2}{\varepsilon_0 V}\sum_{r\in c}\sum_{s\in v}\frac{E_{rs}(F)|\langle\Phi_r(\vec{r})|z|\Phi_s(\vec{r})\rangle|^2}{E_{rs}^2(F)-\hbar^2\Omega^2}. \quad (13)$$

Here, $V=\sqrt{3}N\pi R^2 a$ is the CN volume, $E_{rs}(F)$ are field-dependent eigenvalues of the Hamiltonian matrix, and $\langle\Phi_r(\vec{r})|z|\Phi_s(\vec{r})\rangle=\Sigma_{i,j=1}^{4nN}c_i^{r\,*}c_j^s\langle\varphi_i(\vec{r})|z|\varphi_j(\vec{r})\rangle\approx\Sigma_{i=1}^{4nN}c_i^{r\,*}c_i^s z_i$, where c_i^r, c_j^s are expansion coefficients of the molecular eigenstates in the basis of atomic π orbitals $\varphi_i(\vec{r})$ and the upper summation limit corresponds to the number of atoms in a zigzag CN. Studying a (7,0) CN limited in length to 180 unit cells, the weak-field limit in Eq. (12) is found to be reasonably approximated for $F=0.1$ mV/Å. We compare the approximate analytical result with the full numerical calculation and find virtually indistinguishable results, as demonstrated in Fig. 3. Although the Aspnes perturbation expression has been derived for transitions in the vicinity of the band gap, it is surprisingly good even far from the band gap.

For strong fields, higher-order terms in the expansion of $\chi(F,\omega)$ become important which give rise to oscillating tails

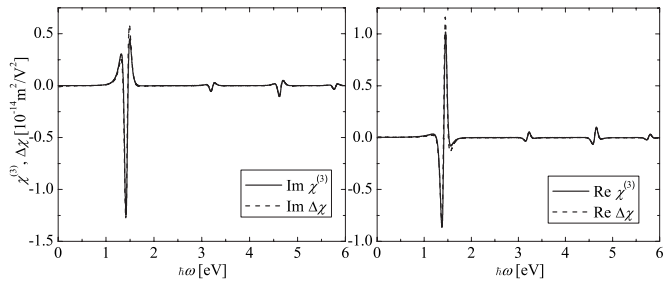

FIG. 3. Comparison of analytical $\chi^{(3)}$ and numerical $\Delta\chi$ results taking $F=0.1$ mV/Å and $\hbar\Gamma=0.1$ eV for a (7,0) CN.

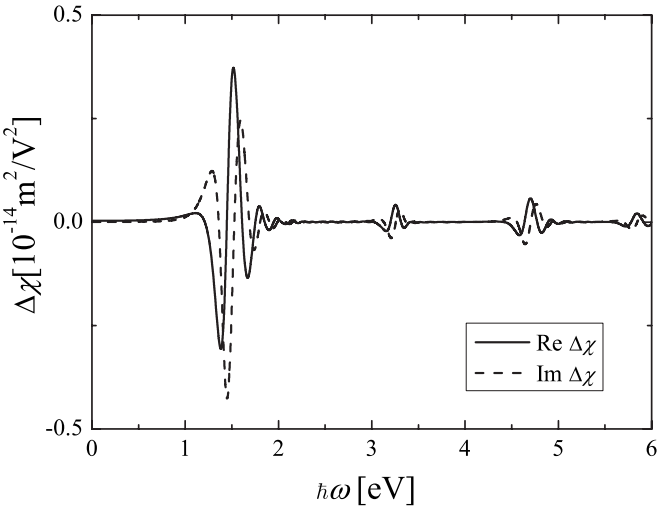

FIG. 4. Numerically obtained $\Delta\chi(F=5.5\ \mathrm{mV/Å})$ for a (7,0) CN taking $\hbar\Gamma=0.1$ eV. The oscillations above the band gap demonstrate that higher-order terms in the expansion of $\chi(F,\omega)$ are significant for such large fields.

of the peaks above the band gap. As an example, Fig. 4 shows a plot of $\Delta\chi(F=5.5\ \mathrm{mV/Å})$. We find that for fields larger than $\sim 1\ \mathrm{mV/Å}$, oscillations above the band gap emerge, which is a characteristic of the nonperturbative Franz-Keldysh regime.[25]

In order to address the possibility of experimental verification of the present results, a number of issues need to be considered. First, experimental samples invariably contain a mixture of CNs differing by diameter and chirality. The precise composition depends on the method of production. Second, the spectral width of all field-induced features is obviously very sensitive to the line broadening Γ. Hence, ideally an experimental sample should be (1) dominated by relatively few CN species and (2) characterized by small line broadening. The latter is typically obtained in micelle-wrapped CNs (Ref. 26) for which broadening as low as $\hbar\Gamma \approx 25-50$ meV has been observed. In this type of samples, the linear absorption of each CN species is clearly resolved and, hence, we clearly believe that the electro-optic response predicted in the present work should be observable as well.

V. CONCLUSIONS

Using a tight-binding model, the quadratic electro-optic (QEO) effect in moderate-gap semiconducting (MS) zigzag CNs has been calculated analytically including contributions from the entire energy band structure. Although the prominent resonance peak of QEO for MS1 is larger than that of MS2 for nearly the same radius, this is not the case for the second peak. Moreover, it is shown that the monotonous increase of the QEO with CN radius within each group of MS is not a general case for all resonance peaks. As a result of the overlap between two energy bands around $k=0$ as well as small reduced effective mass, a large magnitude peak for a small radius CN can appear which is much larger than that of a large radius CN. To assess the applicability of our analytical results obtained in a perturbative approach, a nonperturbative numerical calculation has been performed for comparison. The comparison demonstrates a good agreement between the two approaches for fields weaker than approximately $F=0.1\ \mathrm{mV/Å}$.

*zarifi@physics.aau.dk

[1] M. F. Lin, F. L. Shyu, and R. B. Chen, Phys. Rev. B **61**, 14114 (2000).
[2] G. Ya. Slepyan, S. A. Maksimenko, A. Lakhtakia, O. Yevtushenko, and A. V. Gusakov, Phys. Rev. B **60**, 17136 (1999).
[3] J. Jiang, R. Saito, A. Grüneis, G. Dresselhaus, and M. S. Dresselhaus, Carbon **42**, 3169 (2004).
[4] VI. A. Margulis and E. A. Gaiduk, Chem. Phys. Lett. **341**, 16 (2001).
[5] S. Tasaki, K. Maekawa, and T. Yamabe, Phys. Rev. B **57**, 9301 (1998).
[6] M. Ichida, S. Mizuno, Y. Saito, H. Kataura, Y. Achiba, and A. Nakamura, Phys. Rev. B **65**, 241407(R) (2002).
[7] Z. M. Li, Z. K. Tang, H. J. Liu, N. Wang, C. T. Chan, R. Saito, S. Okada, G. D. Li, J. S. Chen, N. Nagasawa, and S. Tsuda, Phys. Rev. Lett. **87**, 127401 (2001).
[8] S. V. Goupalov, Phys. Rev. B **72**, 195403 (2005).
[9] J. S. Lauret, C. Voisin, G. Cassabois, C. Delalande, P. H. Roussignol, O. Jost, and L. Capes, Phys. Rev. Lett. **90**, 057404 (2003).
[10] J. S. Lauret, C. Voisin, G. Cassabois, C. Delalande, P. H. Roussignol, L. Capes, and O. Jost, Physica E (Amsterdam) **17**, 380 (2003).
[11] J. S. Lauret, C. Voisin, G. Cassabois, J. Tignon, C. Delalande, P. H. Roussignol, O. Jost, and L. Capes, Appl. Phys. Lett. **85**, 3572 (2004).
[12] S. Wang, W. Huang, H. Yang, Q. Gong, Z. Shi, X. Zhou, Di. Qiang, and Z. Gu, Chem. Phys. Lett. **320**, 411 (2000).
[13] X. Liu, J. Si, B. Chang, G. Xu, Q. Yang, Z. Pan, S. Xie, P. Ye, J. Fan, and M. Wan, Appl. Phys. Lett. **74**, 164 (1999).
[14] C. Stanciu, R. Ehlich, V. Petrov, O. Steinkellner, J. Herrmann, I. V. Hertel, G. Ya. Slepyan, A. A. Khrutchinski, S. A. Maksimenko, F. Rotermund, E. E. B. Campbell, and F. Rohmund, Appl. Phys. Lett. **81**, 4064 (2002).
[15] V. A. Margulis and T. A. Sizikova, Physica B **245**, 173 (1998).
[16] VI. A. Margulis, E. A. Gaiduk, and E. N. Zhidkin, Diamond Relat. Mater. **8**, 1240 (1999).
[17] Y. Xu and G. Xiong, Chem. Phys. Lett. **388**, 330 (2004).
[18] Y. Xu and G. Xiong, Physica E (Amsterdam) **25**, 23 (2004).
[19] VI. A. Margulis, E. A. Gaiduk, and E. N. Zhidkin, Phys. Lett. A **258**, 394 (1999).
[20] A. Zarifi and T. G. Pedersen, Phys. Rev. B **74**, 155434 (2006).
[21] D. E. Aspnes and J. E. Rowe, Phys. Rev. B **5**, 4022 (1972).
[22] T. B. Lynge and T. G. Pedersen, Synth. Met. **138**, 329 (2003).
[23] T. G. Pedersen, Phys. Rev. B **67**, 073401 (2003).
[24] A. M. Nemilentsau, G. Y. Slepyan, A. A. Khrutchinskii, and S. A. Maksimenko, Carbon **44**, 2246 (2006).
[25] T. G. Pedersen and T. B. Lynge, Phys. Rev. B **65**, 085201 (2002).
[26] M. J. O'Connell *et al.*, Science **297**, 593 (2002).